# Biosynthesis of Zinc Oxide Nanoparticles using Plant Growth promoting Rhizobacteria of *Curcuma longa* and *Zingiber officinale*

**Mulani Arif A.[1], Bhavikatti Bharati K.[1], Chavan Ranjana S.[2] and Mali Gajanan V.[1,2]***
1. UG and PG Department of Microbiology, Bharati Vidyapeeth's Dr. Patangrao Kadam Mahavidyalaya, Sangli, Maharashtra 416416, INDIA
2. UG and PG Dept. of Microbiology, Bharati Vidyapeeth (Deemed to be University) Yashwantrao Mohite College, Erandwane, Pune, Maharashtra.411038, INDIA
*gajamali@rediffmail.com

***Abstract***
*The biosynthesis of zinc oxide nanoparticles (ZnO NPs) using plant growth-promoting rhizobacteria (PGPR) offers an environmentally acceptable and sustainable alternative to traditional chemical and physical synthesis methods. This work explores the production of ZnO NPs using PGPR isolated from the rhizosphere soil of two medicinal plants Curcuma longa (turmeric) and Zingiber officinale (ginger). The isolated PGPR were characterised by their plant growth-promoting features, including phosphate solubilization, cellulose degradation, zinc solubilization, indole acetic acid (IAA) synthesis and siderophore secretion.*

*Additionally, the screened isolates were tested at various salt concentrations, ranging from 0.5% to 7.5%, to assess their salt stress tolerance. The biosynthesis of ZnO nanoparticles using bacterial isolates was validated by visual monitoring of turbidity changes in reaction mixes containing zinc salts. The formation of turbidity suggested nanoparticle production. The present study demonstrates the successful production of zinc oxide nanoparticles (ZnO NPs) using plant growth-promoting rhizobacteria (PGPR) from Curcuma longa and Zingiber officinale.*

**Keywords:** PGPR, *Curcuma longa, Zingiber officinale,* Biosynthesis, ZnO nanoparticle.

## Introduction

Nanotechnology has gained traction in a variety of scientific sectors including agriculture, health and environmental sciences, with ZnO NPs being particularly recognised for their large surface area, catalytic effectiveness and antibacterial qualities. The biosynthesis of zinc oxide nanoparticles (ZnO NPs) by plant growth-promoting rhizobacteria (PGPR) is an environmentally friendly alternative to traditional chemical and physical synthesis processes, which frequently produce harmful byproducts. Several metabolic steps are involved in PGPR-mediated synthesis including the use of bacterial metabolites, enzymes and proteins as reducing and capping agents for zinc ions. The process begins with metal ion biosorption on the bacterial cell surface, followed by enzymatic reduction which results in nanoparticle nucleation and stability via bacterial proteins and polysaccharides.

This green synthesis approach eliminates the need for harsh chemicals and high-energy inputs, making it a sustainable and environmentally friendly alternative[9,10,16]. Biosynthesised ZnO NPs have shown significant antibacterial activity in medical applications. These nanoparticles, known for their biocompatibility and powerful antibacterial activity, successfully battle clinical pathogens such as multidrug-resistant bacteria, making them intriguing candidates for novel antimicrobial therapeutics. Their mode of action involves breaking bacterial cell membranes, producing reactive oxygen species and interfering with DNA replication, suggesting a viable strategy for combating antibiotic resistance[11,12,15].

ZnO NPs have shown significant potential in drug delivery[13]. These biosynthesised nanoparticles have shown strong cytotoxic effects on HeLa cell lines, cervical cancer[14] and breast cancer treatment[2] indicating their promise in cancer treatment. They are selectively harmful to cancer cells and have negligible effects on healthy cells. Furthermore, ZnO NPs manufactured in a green technique with *Zingiber officinale* (ginger) extracts use the plant's natural phytochemicals to decrease and stabilise zinc ions, resulting in nanoparticle formation[5].

The positive impacts of plant growth-promoting rhizobacteria (PGPR) on plant health, such as nutrient solubilization, phytohormone synthesis and biocontrol mechanisms, have been extensively researched through a variety of mechanisms, including phosphate solubilization, indole acetic acid (IAA) synthesis and siderophore secretion. These bacteria invade the rhizosphere and stimulate plant growth[1,8]. The potential of PGPR in the biosynthesis of metal oxide nanoparticles has also been investigated recently, offering an environmentally responsible and sustainable method of producing nanomaterials[16]. The utilisation of PGPR in the biosynthesis of zinc oxide nanoparticles (ZnO NPs) not only enhances the stability and functional properties of the nanoparticles but also contributes to plant growth and stress tolerance.

Several PGPR genera including *Bacillus, Pseudomonas, Azospirillum and Rhizobium*, facilitate the synthesis of ZnO NPs, which play a crucial role in strengthening plant defence mechanisms. The combined application of ZnO NPs and PGPR has been shown to enhance antioxidant enzyme activities, including superoxide dismutase (SOD), catalase (CAT) and peroxidase (POD), thereby maintaining cellular

homeostasis and reducing oxidative damage under environmental stress conditions. In agricultural systems, this synergistic approach has demonstrated effectiveness in enhancing soil enzyme activity, optimising biochemical metabolism and improving plant resilience to abiotic stresses such as drought, heat and salinity. For instance, studies on wheat cultivated under saline irrigation have reported improved plant productivity and stress tolerance when ZnO NPs are applied in conjunction with PGPR[4].

Zinc oxide (ZnO) nanoparticles produced from plant extracts and plant growth-promoting rhizobacteria (PGPR) have shown great promise in agricultural applications. These biosynthesised nanoparticles act as nano fertilisers, promoting plant growth, boosting crop yields and improving disease resistance. One of their primary environmental benefits is increased nutrient uptake and efficiency, notably for zinc, an important mineral for plant metabolism. Field investigations have indicated that using these nanoparticles can boost agricultural yields by 15-25%, depending on the crop variety and weather conditions. Furthermore, their use stimulates better root development and biomass accumulation, which contributes to overall plant vitality.

Furthermore, ZnO nanoparticles have antibacterial capabilities that aid in minimising pathogen incidence, particularly soil-borne plant diseases. These nanoparticles require lower application rates than conventional fertilisers, reducing potential environmental effects such as soil damage and nutrient runoff. Their incorporation into agricultural practices is especially beneficial for combating zinc deficiency in soils, a global problem that affects nearly half of cultivated lands. ZnO nanoparticles provide a long-term solution for boosting plant health and productivity by reducing biotic stress and increasing nutrient availability[6]. Overall, this eco-friendly and sustainable strategy presents a promising avenue for enhancing agricultural resilience while advancing the development of environmentally responsible nanotechnology.

Recent research highlights the potential of biosynthesising zinc oxide nanoparticles (ZnO NPs) using *Curcuma longa* and plant growth-promoting rhizobacteria (PGPR) as an effective strategy for enhancing bioactive compound content and antibacterial properties in *Curcuma longa*[3]. Furthermore, the incorporation of ZnO NPs into plant cultivation has been shown to enhance growth parameters and modify bioactive component profiles, thereby improving the production of therapeutic compounds in *Curcuma longa*[2].

This study focuses on the biosynthesis of ZnO NPs using PGPR isolated from the rhizospheric soil of two medicinal plants, *Curcuma longa* (turmeric) and *Zingiber officinale* (ginger), both of which are widely recognised for their medicinal properties and significance in traditional medicine. The research aims to isolate and characterise PGPR from the rhizosphere, to assess their plant growth-promoting traits and to evaluate their efficacy in ZnO NP biosynthesis.

Additionally, the study examines the physicochemical properties of the synthesised ZnO NPs and explores their potential applications in agriculture and biomedicine.

## Material and Methods

**Collection of Soil Sample:** Soil samples were collected from the rhizospheric region of medicinal plants in the Sangli district, Maharashtra. Two samples of *Curcuma longa* (Turmeric) were collected from Karandwadi (16°56’21.71” N, 74°27’30.83” E and 16°56’10.60” N, 74°27’52.54” E) and one sample from Kavathepiran (16°52’57.81” N, 74°27’54.73” E). Samples of *Zingiber officinale* (Ginger) were collected from Burungwadi (17°01’71.71” N, 74°51’24.539” N), Vasagade (16°58’40” N, 74°30’36” E) and Wangi (17°23’68.47” N, 74°43’25.944” E). The geographic coordinates were recorded using the Digital Compass application. According to Garcia et al[7], soil samples were taken from the rhizosphere at a depth of roughly 20 cm. After being promptly sealed, appropriately labeled and packed in sterile plastic bags, the samples were taken to the microbiology lab for additional examination. The following labels were applied to the soil samples: ginger samples (G1, G2, G3) and turmeric samples (T1, T2, T3).

**Physicochemical Analysis of Soil:** The collected soil samples were analyzed for organic carbon, nitrogen, phosphorus, potassium and pH. Organic carbon was analyzed using the Walkley method[19]. Available nitrogen was analyzed using the Kjeldahl method. Available phosphorus was analyzed using Bray’s P-1 method. Available potassium was analysed using the ammonium acetate method and pH was measured using a digital pH meter.

**Plant Growth-Promoting Rhizobacteria (PGPR) Isolation:** 1 g sample of soil was serially diluted up to $10^{-6}$ after being inoculated in 10 mL of sterile distilled water. Each diluted sample was scattered onto sterile nutrient agar plates in a 0.1 mL aliquot and the plates were then incubated for 24 hours at room temperature (R.T.). Eight colonies in all were chosen for additional research, purified on nutrient agar plates and then cultured in the same manner. The isolate’s morphological characteristics were documented. The biochemical characteristics of isolates were also examined for the amylase, caseinase, catalase and formation of hydrogen sulphide.

**PGPR screening**

**a) Phosphate Solubilization:** After being spot-inoculated, isolated colonies were cultured for 24 to 48 hours at R.T. Phosphate solubilization ability was demonstrated by the presence of a halo zone[8]. The following formula was used to determine the phosphate solubilization index (SI):

S I = colony diameter + halo zone diameter/ colony diameter

**b) Cellulose Degradation:** For 48 hours, carboxymethyl cellulose agar was spot-inoculated with a loopful of bacterial suspension and incubated at room temperature. A clear hydrolysis zone around the colony suggested cellulose breakdown. The ratio of the hydrolysis zone diameter (D) to the bacterial colony diameter (d) was used to calculate the cellulase activity.

**c) Zinc Solubilization:** The isolates were cultured for 48 hours at room temperature after being inoculated into a minimum salt medium containing 0.1% zinc oxide. The development of a transparent halo zone indicated zinc solubilization[18].

**d) Production of Indole Acetic Acid (IAA):** Bacterial isolates were inoculated in a broth containing 5 millilitres of tryptone/peptone yeast extract and incubated for 72 hours at room temperature. Following incubation, 1.5 mL of the culture was centrifuged for 10 minutes at 12,850 × g. After adding 1 mL of Salkowski reagent (50 mL of 35% perchloric acid and 1 mL of 0.5 M $FeCl_3$ solution) to the supernatant, it was allowed to sit at room temperature in the dark for an hour. IAA production was denoted by a red coloring[17]. A standard curve with known IAA values (0–100 µg/mL) was used to calculate IAA concentrations.

**e) Production of Siderophores:** Isolates were cultured at room temperature for 48 hours after being spot-inoculated onto Chrome Azurol S (CAS) agar plates. Siderophore production was indicated by the existence of a halo zone.

**f) Ammonia Production:** After inoculating 4% peptone broth, isolates were cultured for 72 hours at room temperature. Nessler's reagent (1 mL) was added following incubation. Ammonia production was indicated by a yellow to brown precipitate[8].

**Study on the effect of salt concentration on the growth of the isolates:** The isolates were further tested for their reaction to environmental variables, including salt tolerance. The isolates were inoculated into nutrient broth enriched with 0.5%, 1.5%, 2.5%, 5.0% and 7.5% NaCl and incubated at R.T. for 24 hours separately.

**Extracellular nanoparticle synthesis:** Bacterial suspensions were inoculated into the nutrient broth and incubated at R.T. on a rotary shaker for 24 hours. The culture was centrifuged at 1000 rpm for 10 minutes and the supernatant was collected. Equal volumes of 0.250 mM zinc nitrate and zinc sulfate solutions were added. The mixture was incubated at R.T. for 24 hours until turbidity developed. The solution was centrifuged at 8000 rpm for 10 minutes, washed three times with double-distilled water and subjected to a final wash with 70% ethanol[12]. The purified sample was dried in an oven at 80°C.

**Statistical Analysis:** All experiments were conducted in triplicate to ensure reproducibility.

## Results and Discussion

**Physicochemical characteristics of soil:** The physicochemical analysis of soil samples collected from the rhizosphere of *Curcuma longa* (named as T1, T2, T3) (Table 1) and *Zingiber officinale* (named as G1, G2, G3) (Table 1) from different sites revealed variations in soil pH, nutrient content and mineral composition. The soil pH ranged from 7.19 to 8.12, indicating a slightly alkaline nature, especially in *Curcuma longa* samples. Potassium levels exhibited significant variation, whereas phosphorus and nitrogen levels were relatively lower in some samples, suggesting potential nutrient deficiencies. The soil pH ranged from 7.19 to 8.12, indicating a somewhat alkaline environment.

Among the macronutrients studied, nitrogen concentration was found to be highest in G1 (336 kg/h) and lowest in G3. Phosphorus levels were between 34 kg/h in T3 and 104 kg/h in T2. G3 had the highest potassium concentration (685 kg/h), whereas G2 had the lowest (73 kg/h). Organic carbon content also varied, with the highest quantity found in G2 (0.34%) and the lowest in G3 (0.14%). Micronutrient studies found significant differences in iron, manganese, zinc and copper levels. The maximum zinc concentration was detected in T3 (0.62 ppm), while the lowest was discovered in G3 (0.04 ppm) (Table 1).

**Isolation and Characterization of bacterial isolates:** Eight bacterial isolates were obtained from the soil samples and characterized based on their morphological and biochemical properties. Variations were observed in colony characteristics, motility and enzymatic activities and hydrogen sulphide formation.

**a) Morphological Analysis:** The bacterial colonies showed predominantly circular shapes with well-defined regular margins. Most isolates exhibited a moist consistency and their pigmentation ranged from off-white to translucent (Table 2).

**b) Gram Staining and Motility:** The majority of bacterial isolates were characterized as Gram-negative rods. Additionally, three isolates, G12, G20 and G30, were identified as non-motile (Table 3).

**c) Biochemical Characterization:** The biochemical characterisation of amylase, caseinase and catalase activity exhibited the absence of enzymatic activity and none of the isolates demonstrated the ability to produce hydrogen sulfide.

**Screening of PGPR Isolates**

**Phosphate solubilization activity:** The bacterial isolate's capacity to promote plant development was assessed using a variety of functional screening assays. All isolates showed phosphate solubilization activity, with isolate T30 having the highest solubilization index of 13, followed by T11 of 8.33 (Table 4, Photoplate 1, Figure 1).

**Cellulose degradation:** Cellulose breakdown was confirmed in isolate T30, as demonstrated by the clear zone (Photoplate 2).

**Zinc solubilization:** Zinc solubilization was found in isolates G12, T20 and T30, resulting in distinct halos around the colonies (Photoplate 3).

**Indole acetic acid production:** Colourimetric examination showed indole acetic acid (IAA) synthesis, with isolates G30 and T12 having the highest quantities (Tables 5 and 6, Photoplate 4, Figure 2).

**Siderophore production:** In addition, isolates G11, G12, T11 and T12 produced siderophores, indicating that they may play a role in increasing iron availability (Photoplate 5). Notably, none of the isolates produced ammonia, indicating a restricted role in nitrogen metabolism.

**Study on the effect of salt concentration on the growth of the isolates:** All isolates exhibited moderate tolerance to salt, though their growth progressively declined at higher salt concentrations (Table 7) (Figure 3).

**Table 1**
**Physicochemical characteristics of soil**

| S.N. | Parameter | Soil sample code | | | | | |
|---|---|---|---|---|---|---|---|
| | | G1 | G2 | G3 | T1 | T2 | T3 |
| 1. | pH | 7.5 | 7.24 | 7.19 | 7.5 | 7.61 | 8.12 |
| 2. | E. C. (mmhos/cm) | 0.182 | 0.23 | 0.211 | 0.211 | 0.332 | 0.263 |
| 3. | Nitrogen (kg/h) | 336 | 328 | 255 | 276 | 296 | 313 |
| 4. | Phosphorus (kg/h) | 98 | 89 | 85 | 45 | 104 | 34 |
| 5. | Potassium (kg/h) | 94 | 73 | 685 | 282 | 672 | 242 |
| 6. | Calcium (meq%) | 20 | 22 | 16 | 14 | 19 | 19 |
| 7. | Magnesium (meq%) | 3 | 13 | 7 | 8 | 6 | 9 |
| 8. | Free lime (%) | 5.12 | 3.9 | 3.66 | 4.94 | 5.38 | 4.78 |
| 9. | Organic Carbon(%) | 0.32 | 0.34 | 0.14 | 0.15 | 0.2 | 0.3 |
| 10. | Iron (ppm) | 0.03 | 0.34 | 0.04 | 0.39 | 0.03 | 0.02 |
| 11. | Manganese (ppm) | 0.37 | 0.37 | 0.24 | 0.37 | 0.36 | 0.26 |
| 12. | Zinc (ppm) | 0.18 | 0.08 | 0.04 | 0.52 | 0.04 | 0.62 |
| 13. | Copper (ppm) | 0.06 | 0.37 | 0.07 | 0.11 | 0.05 | 0.05 |

**Table 2**
**Morphological characteristics of screened bacterial isolates colonies**

| S.N. | Isolate | Size (mm) | Shape | Margin | Elevation | Opacity | Colour | Consistency |
|---|---|---|---|---|---|---|---|---|
| 1 | G11 | 2 | Circular | Regular | Flat | Transluscent | Off White | Moist |
| 2 | G12 | 1 | Circular | Regular | Flat | Opaque | Off White | Moist |
| 3 | G20 | 2 | Circular | Regular | Flat | Opaque | White | Moist |
| 4 | G30 | 1 | Circular | Regular | Raised | Transluscent | Colourless | Moist |
| 5 | T11 | 2 | Circular | Regular | Raised | Transluscent | White | Moist |
| 6 | T12 | 2 | Circular | Regular | Flat | Opaque | White | Moist |
| 7 | T20 | 1 | Circular | Regular | Flat | Transluscent | White | Moist |
| 8 | T30 | 1 | Circular | Regular | Flat | Opaque | White | Moist |

**Table 3**
**Gram nature and motility of screened bacterial isolates**

| S.N. | Isolate | Gram Nature | Motility |
|---|---|---|---|
| 1 | G11 | Gram-negative short rods | Motile |
| 2 | G12 | Gram-positive rods | Non Motile |
| 3 | G20 | Gram-negative short rods | Non Motile |
| 4 | G30 | Gram-negative short rods | Non Motile |
| 5 | T11 | Gram-negative short rods | Motile |
| 6 | T12 | Gram-negative rods | Motile |
| 7 | T20 | Gram-negative short rods | Motile |
| 8 | T30 | Gram-negative short rods | Motile |

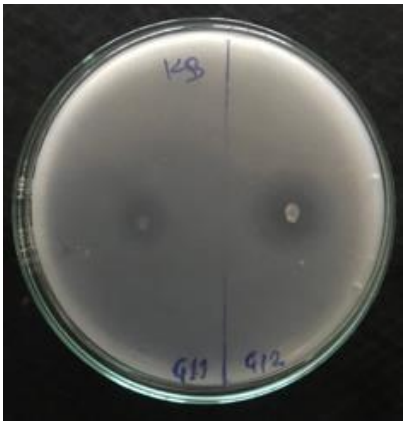


**Isolate G11 and G12**

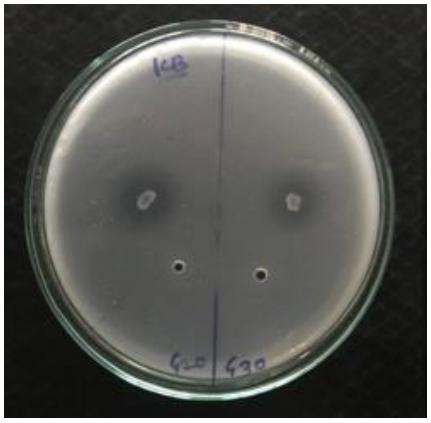


**Isolate G20 and G30**

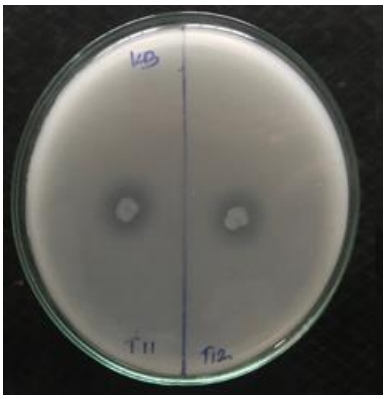


**Isolate T11 and T12**

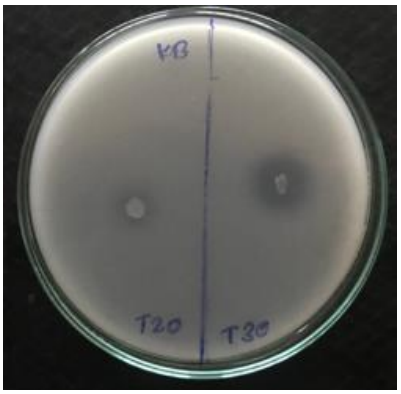


**Isolate T20 and T30**

**Photoplate 1: Phosphate solubilization on Katznelson and Bose medium**

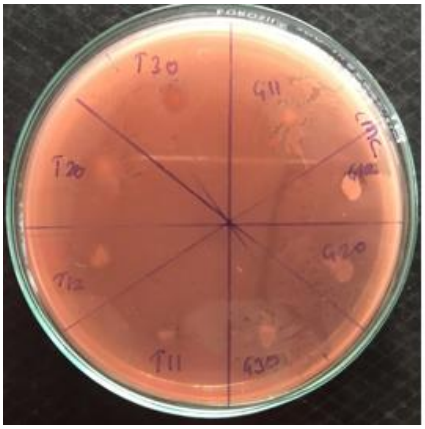


**Photoplate 2: Cellulose degradation by isolates**

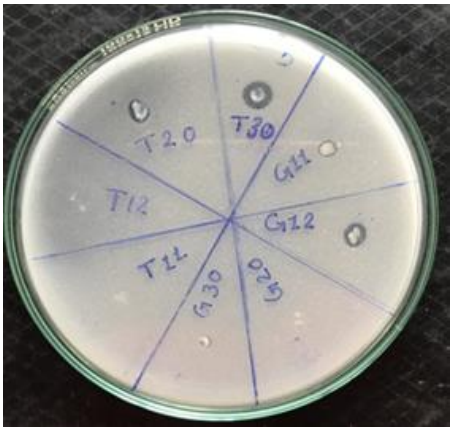


**Photoplate 3: Zinc solubilization by isolates**


**Photoplate 4: Indole acetic acid production by isolates**

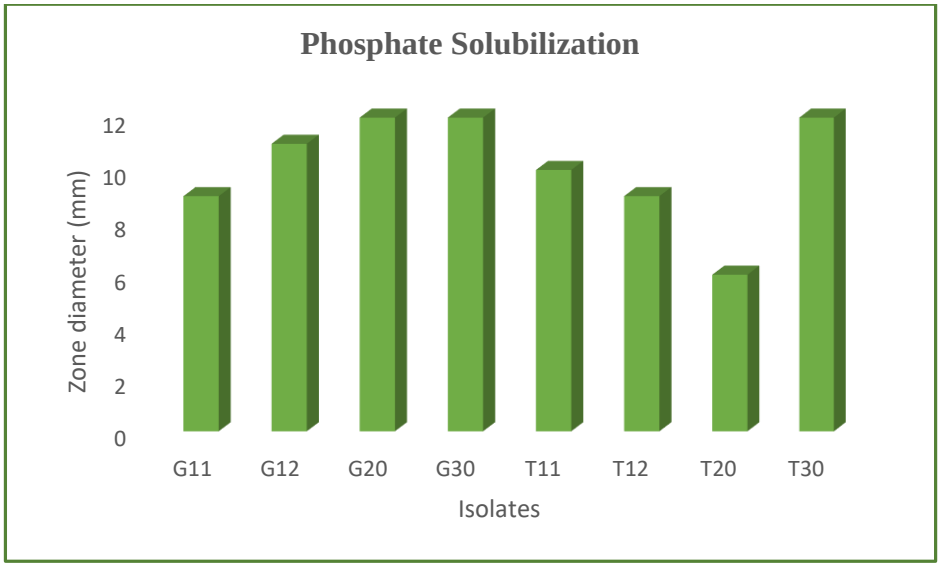


**Figure 1: Graphical representation of the phosphate solubilization index of the isolates**

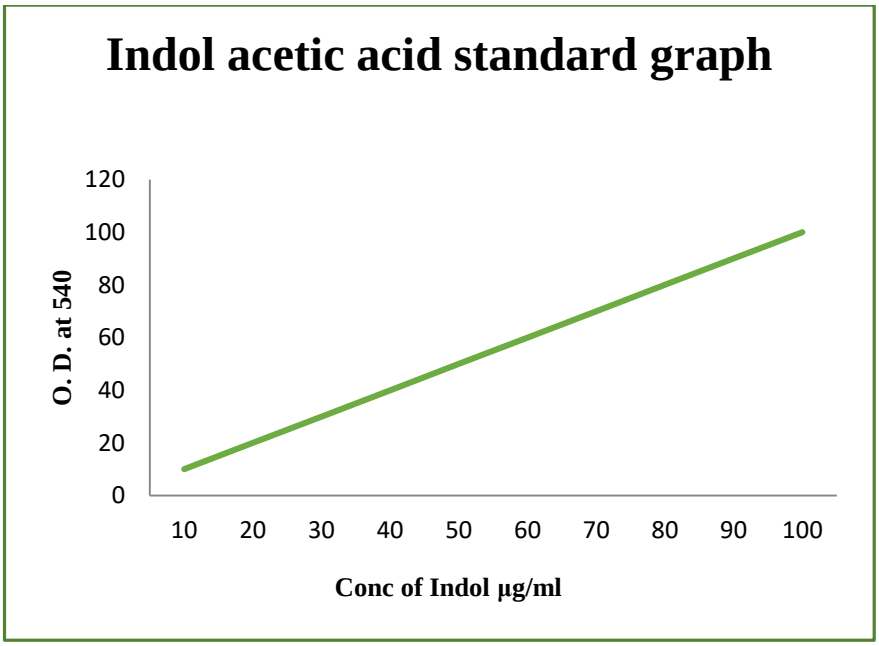


**Figure 2: Graphical presentation of Standard IAA acetic acid**

**Table 4**
**Phosphate solubilization index of the isolates**

| S.N. | Isolate | Colony diameter (mm) | Zone diameter (mm) | Phosphate Solubilization Index |
|---|---|---|---|---|
| 1 | G11 | 3 | 9 | 4 |
| 2 | G12 | 3 | 11 | 6.66 |
| 3 | G20 | 3 | 12 | 7 |
| 4 | G30 | 3 | 12 | 7 |
| 5 | T11 | 5 | 10 | 8.33 |
| 6 | T12 | 6 | 9 | 7.5 |
| 7 | T20 | 3 | 6 | 5 |
| 8 | T30 | 2 | 12 | 13 |

Table 7 shows the effects of various salt concentrations (0.5% to 7.5%) on bacterial isolates as assessed by optical density (OD) at 540 nm. The results show that when salt concentration increases, OD values decrease, indicating that bacterial growth is reduced owing to osmotic stress. G11, G12 and T12 demonstrated greater tolerance at lower salt concentrations but experienced a considerable drop in OD at 7.5%. G20, T11 and T20 had lower OD values, indicating

lesser salt tolerance. Most isolates showed a significant decrease in growth at 5% and 7.5% salt concentrations, indicating their susceptibility to high salinity.

**Extracellular ZnO Nanoparticle Synthesis:** The biosynthesis of ZnO nanoparticles using bacterial isolates was validated by visual monitoring of turbidity changes in reaction mixes containing zinc salts. The formation of turbidity suggested nanoparticle production. (Photoplate 6).

## Discussion

The biosynthesis of zinc oxide nanoparticles (ZnO NPs) with plant growth-promoting rhizobacteria (PGPR) offers a sustainable, environmentally friendly method for nanoparticle production. The resulting crystalline, stable and antibacterial nanoparticles are suitable for agricultural and biological applications, with future research focusing on scalability and functional optimisation.

**Table 5**
**Indole acetic acid production standard**

| S.N. | Stock | Distilled water | Total conc. µg/ml | O. D. at 540 |
|---|---|---|---|---|
| 1. | 1 | 9 | 10 | 0.06±0.325 |
| 2. | 2 | 8 | 20 | 0.15±0.214 |
| 3. | 3 | 7 | 30 | 0.23±0.265 |
| 4. | 4 | 6 | 40 | 0.33±0.215 |
| 5. | 5 | 5 | 50 | 0.36±0.258 |
| 6. | 6 | 4 | 60 | 0.39±0.214 |
| 7. | 7 | 3 | 70 | 0.39±0.364 |
| 8. | 8 | 2 | 80 | 0.46±0.254 |
| 9. | 9 | 1 | 90 | 0.48±0.214 |
| 10. | 10 | 0 | 100 | 0.5±0.215 |

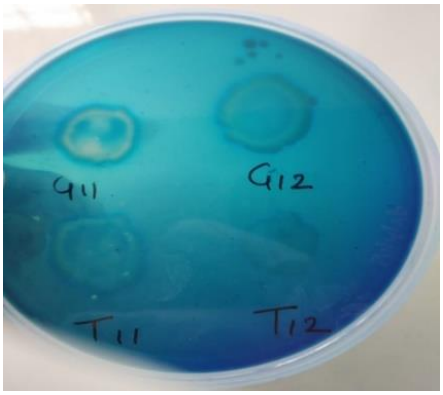


**Photoplate 5: Siderophore production by isolates**

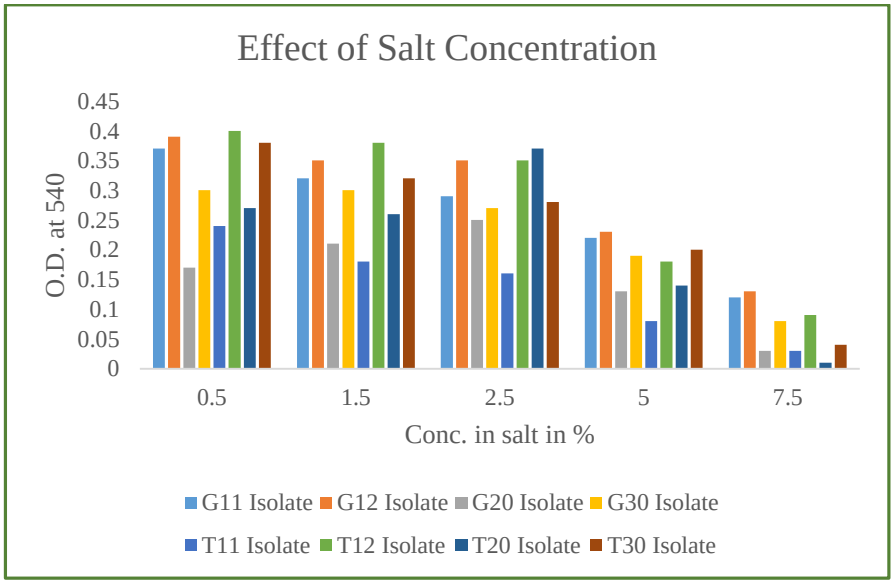


**Figure 3: Effect of salt concentration on the growth of the isolates**

**Table 6**
**Indole acetic acid production by isolates**

| S.N. | Isolate | Concentration of Indole Acetic Acid µg/ml | O. D. at 540 |
|---|---|---|---|
| 1 | G11 | 60 | 0.44±0.964 |
| 2 | G12 | 54 | 0.39±0.258 |
| 3 | G20 | 57 | 0.34±0.621 |
| 4 | G30 | 75 | 0.55±0.341 |
| 5 | T11 | 49 | 0.35±0.127 |
| 6 | T12 | 74 | 0.54±0.214 |
| 7 | T20 | 71 | 0.52±0.042 |
| 8 | T30 | 71 | 0.52±0.214 |

**Table 7**
**Effect of salt concentration and graphical presentation**

| S.N. | Isolate | Conc of salt in % and OD at 540 | | | | |
|---|---|---|---|---|---|---|
| | | 0.5 | 1.5 | 2.5 | 5 | 7.5 |
| 1 | G11 | 0.37±0.254 | 0.32±0.324 | 0.29±0.365 | 0.22±0.325 | 0.12±0.325 |
| 2 | G12 | 0.39±0.351 | 0.35±0.215 | 0.35±0.985 | 0.23±0.214 | 0.13±0.145 |
| 3 | G20 | 0.17±0.258 | 0.21±0.324 | 0.25±0.248 | 0.13±0.352 | 0.03±0.254 |
| 4 | G30 | 0.3±0.124 | 0.3±0.201 | 0.27±0.365 | 0.19±0.562 | 0.08±0.321 |
| 5 | T11 | 0.24±0.324 | 0.18±0.210 | 0.16±0.125 | 0.08±0.321 | 0.03±0.225 |
| 6 | T12 | 0.4±0.236 | 0.38±0.362 | 0.35±0.365 | 0.18±0.124 | 0.09±0.332 |
| 7 | T20 | 0.27±0.415 | 0.26±0.254 | 0.37±0.215 | 0.14±0.254 | 0.01±0.254 |
| 8 | T30 | 0.38±0.245 | 0.32±0.215 | 0.28±0.124 | 0.2±0.124 | 0.04±0.215 |

***Note:** ± indicates standard deviation

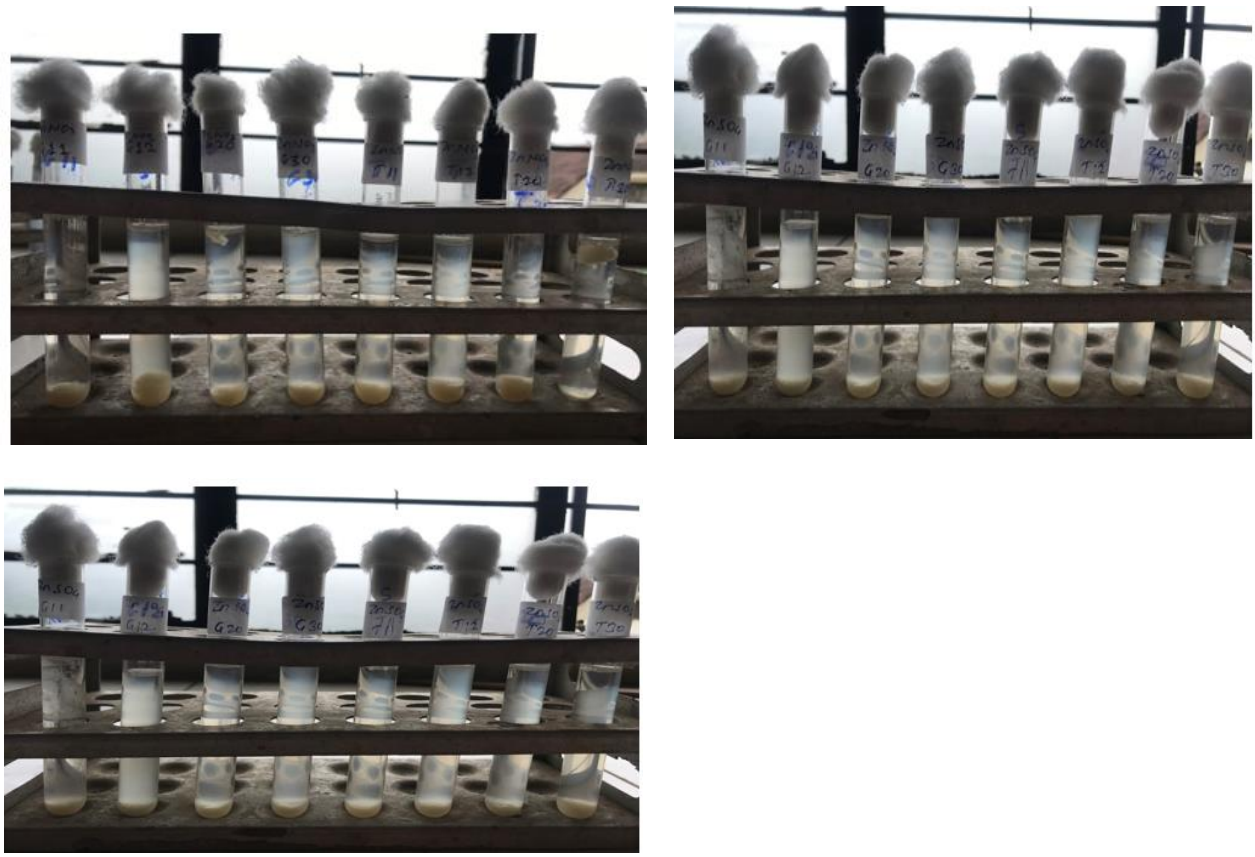

**Photoplate 6: Zn oxide nanoparticles synthesis- visual detection**

The study by Anand and Jayalakshmy[6] explores the biogenic synthesis of ZnO nanoparticles using the aqueous root extracts of *Zingiber officinale*, which are rich in flavonoids. The resulting nanoparticles have an average size of 30-50nm

and a strong absorbance in the 1600-1450cm-1 range, making them an eco-friendly alternative to chemical synthesis.

The study by Aldayel[3] investigates the effects of zinc oxide nanoparticles on the bioactive component compositions of *Curcumin longa*, a plant species. The researchers treated *C. longa* leaves with different doses of ZnO NPs, resulting in increased levels of bisdemethoxycurcumin, demethoxycurcumin and curcumin in ethanolic extracts. The results showed that *C. long* ZnO-NPs displayed antibacterial activity against *S. aureus* and *P. aeruginosa* strains, but little against *E. coli*. Time-kill studies showed that ZnO-NPs at 4 MIC killed *P. aeruginosa*, *A. baumannii* and *Bacillus sp.* after 2 hours. The strongest antibacterial activity was observed with the extract from plantlets grown without nanoparticles.

The study by Alharbi et al[4] found that combining PGPR and ZnO-NPs effectively protected wheat plants from saline water irrigation by increasing antioxidant enzyme activities and $K^+$ uptake. This led to a significant reduction in electrolyte leakage, proline, MDA and $H_2O_2$ levels, increased N uptake and increased soil urease and dehydrogenase activity.

## Conclusion

The current study demonstrates the successful production of zinc oxide nanoparticles (ZnO NPs) using plant growth-promoting rhizobacteria (PGPR) from *Curcuma longa* and *Zingiber officinale*. The microbial-mediated synthesis of ZnO NPs provides an environmentally acceptable, cost-effective and long-lasting alternative to traditional chemical and physical processes. The synthesised nanoparticles had promising physicochemical properties indicating possible uses in agriculture, medicine and environmental remediation. Furthermore, the involvement of PGPR in improving plant health and nanoparticle stability emphasises the importance of microbial nanotechnology.

Future studies should concentrate on optimising synthesis parameters and investigating the molecular elements of microbial nanoparticle production for large-scale applications. This study highlights the potential of PGPR isolates from the rhizosphere of *Curcuma longa* and *Zingiber officinale* in promoting plant growth and biosynthesising ZnO nanoparticles. The isolates exhibited significant phosphate solubilization, IAA production and zinc solubilization abilities, demonstrating their relevance in sustainable agriculture and nanotechnology. Ongoing research focuses on nanoparticle characterisation and their potential applications in soil health improvement and eco-friendly agricultural practices.

## Acknowledgement

The authors are thankful to Principal, Bharati Vidyapeeth's Dr Patangrao Kadam Mahavidyalaya, Sangli, for his support.

## References

1. Ahmad A., Senapati S., Khan M.I., Kumar R., Ramani R., Srinivas V. and Sastry M., Intracellular synthesis of gold nanoparticles by a novel alkalotolerant actinomycete, Rhodococcus species, *Nanotechnology*, **14(7)**, 824–828, https://doi.org/10.1088/0957-4484/14/7/323 **(2003)**

2. Alallam B., Doolaanea A.A., Alfatama M. and Lim V., Phytofabrication and Characterisation of Zinc Oxide Nanoparticles Using Pure Curcumin, *Pharmaceuticals*, **16(2)**, https://doi.org/10.3390/ph16020269 **(2023)**

3. Aldayel M.F., Enhancement of the Bioactive Compound Content and Antibacterial Activities in Curcuma Longa Using Zinc Oxide Nanoparticles, *Molecules*, **28(13)**, https://doi.org/10.3390/molecules28134935 **(2023)**

4. Alharbi K., Hafez E.M., Omara A.E.D., Rashwan E. and Alshaal T., Zinc oxide nanoparticles and PGPR strengthen salinity tolerance and productivity of wheat irrigated with saline water in sodic-saline soil, *Plant and Soil*, **493(1–2)**, 475–495, https://doi.org/10.1007/s11104-023-06245-7 **(2023)**

5. Ambawade Mukund S., Patil Dipak D., Pathade Girish R. and Mali Gajanan V., Indole acetic acid (IAA) production by endophytic bacterial isolate Agrobacterium tumefaciens BE-1 from roots of Musa acuminata, *Res. J. Biotech.*, **19(4)**, 32-39, https://doi.org/10.25303/1904rjbt032039 **(2024)**

6. Anand Raj L.F.A. and Jayalakshmy E., Biosynthesis and characterization of zinc oxide nanoparticles using root extract of Zingiber officinale, *Oriental Journal of Chemistry*, **31(1)**, 51–56, https://doi.org/10.13005/ojc/310105 **(2015)**

7. Garcia C., Roldan A. and Hernandez T., Ability of different plant species to promote microbiological processes in semiarid soil, *Geoderma*, **124(1–2)**, 193–202, https://doi.org/10.1016/j.geoderma.2004.04.013 **(2005)**

8. Glick B.R., Plant Growth-Promoting Bacteria: Mechanisms and Applications, *Scientifica*, https://doi.org/10.6064/2012/963401 **(2012)**

9. Li X., Xu H., Chen Z.S. and Chen G., Biosynthesis of nanoparticles by microorganisms and their applications, *Journal of Nanomaterials*, https://doi.org/10.1155/2011/270974 **(2011)**

10. Murali M., Gowtham H.G., Shilpa N., Singh S.B., Aiyaz M., Sayyed R.Z., Shivamallu C., Achar R.R., Silina E., Stupin V., Manturova N., Shati A.A., Alfaifi M.Y., Elbehairi S.E.I. and Kollur S.P., Zinc oxide nanoparticles prepared through microbial mediated synthesis for therapeutic applications: a possible alternative for plants, *Frontiers in Microbiology*, **14**, 1–20, https://doi.org/10.3389/fmicb.2023.1227951 **(2023)**

11. Narayanan P.M., Wilson W.S., Abraham A.T. and Sevanan M., Synthesis, Characterization and Antimicrobial Activity of Zinc Oxide Nanoparticles Against Human Pathogens, *BioNanoScience*, **2(4)**, 329–335, https://doi.org/10.1007/s12668-012-0061-6 **(2012)**

12. Patil S.C., Dhavale R.P., Patil V.L., Nimbalkar M.S., Sonawane K.D., Patil P.S., Karanjkar M.M. and Pawar K.D., Calcination temperatures influence the chemo-resistive gas sensing properties of biogenic zinc oxide nanoparticles with antibacterial

activity, *Inorganic Chemistry Communications*, **153**, 110847, https://doi.org/10.1016/j.inoche.2023.110847 **(2023)**

13. Patra J.K., Das G., Fraceto L.F., Campos E.V.R., Rodriguez-Torres M.D.P., Acosta-Torres L.S., Diaz-Torres L.A., Grillo R., Swamy M.K., Sharma S., Habtemariam S. and Shin H.S., Nano based drug delivery systems: Recent developments and future prospects, *Journal of Nanobiotechnology*, **16(1)**, 1–33, https://doi.org/10.1186/s12951-018-0392-8 **(2018)**

14. Perumal P., Sathakkathulla N.A., Kumaran K., Ravikumar R., Selvaraj J.J., Nagendran V., Gurusamy M., Shaik N., Gnanavadivel Prabhakaran S., Suruli Palanichamy V., Ganesan V., Thiraviam P.P., Gunalan S. and Rathinasamy S., Green synthesis of zinc oxide nanoparticles using aqueous extract of shilajit and their anticancer activity against HeLa cells, *Scientific Reports*, **14(1)**, 1–11, https://doi.org/10.1038/s41598-024-52217-x **(2024)**

15. Rajamanickam U., Viswanathan S. and Muthusamy P., Biosynthesis of Zinc Nanoparticles Using Actinomycetes for Antibacterial Food Packaging, International Conference on Nutrition and Food Sciences, **39**, 195–199 **(2012)**

16. Saberi Riseh R. and Gholizadeh Vazvani M., Green synthesis of metal nanoparticles using plant growth promoting rhizobacteria and application in agriculture, *Plant Nano Biology*, **10**, 100111, https://doi.org/10.1016/j.plana.2024.100111 **(2024)**

17. Sarwar M. and Kremer R.J., Determination of bacterially derived auxins using a microplate method. Letters in applied microbiology, *Letters in Applied Microbiology*, **20(5)**, 282–285 **(1995)**

18. Sivaraj Saravanan V., Rama Subramoniam S. and Anthoni Raj S., Assessing *in Vitro* Solubilization Potential of Different Zinc Solubilizing Bacterial (Zsb) Isolates, *Brazilian Journal of Microbiology*, **34**, 121–125 **(2003)**

19. Walkley A. and Black C.A., Organic Carbon: Methods of Soil Analysis (parts 1 and 2), Agronomy, American Society of Agronomy, Inc., Madison, 849–865 **(1965)**.

(Received 20th June 2025, accepted 01st August 2025)